Available online at www.sciencedirect.com

SCIENCE DIRECT

Metabolism Clinical and Experimental 54 (2005) 619–627

Metabolism
Clinical and Experimental

www.elsevier.com/locate/metabol

Synthetic protease inhibitor camostat prevents and reverses dyslipidemia, insulin secretory defects, and histological abnormalities of the pancreas in genetically obese and diabetic rats

Dongmei Jia, Masashi Taguchi, Makoto Otsuki*

Third Department of Internal Medicine, University of Occupational and Environmental Health, Japan, School of Medicine, Kitakyushu 807-8555, Japan

Received 3 April 2004; accepted 17 December 2004

Abstract

Background: Otsuka Long-Evans Tokushima Fatty (OLETF) rat, a model of type 2 diabetes, lacks the expression of cholecystokinin-1 receptor mRNA and exhibits inflammation and degeneration of the pancreas and eventually develops insulinopenic diabetes. Protease inhibitors are known to modulate inflammatory response and fibrosis as well as inhibit proteases activity.

Aim: To examine the effects of long-term treatment with camostat, a synthetic protease inhibitor, on metabolic and histopathological changes in the islets of OLETF rats.

Method: OLETF rats were fed either camostat-containing food (200 mg/100 g) from 12 or 28 weeks of age to 72 weeks of age, or fed standard rat diet.

Results: Camostat-fed rats gained less weight or lost weight, although they consumed more food than the control rat when food intake was adjusted for body weight. Camostat reduced visceral adipose depots and fasting serum concentrations of triglyceride, free fatty acids, cholesterol, glucose, and insulin. Pancreatic insulin content in camostat-treated rats was significantly higher than in control rats. Immunohistochemistry revealed marked suppression of expressions of tumor necrosis factor α, interleukin 1β, interleukin 6, and α-smooth muscle actin in the islets of camostat-treated rats, compared with control rats. Histologically, disruption of the islets and pancreatic fibrosis were noted in control rats but not in camostat-fed rats.

Conclusion: Our findings suggest that camostat prevents and reverses obesity, hyperinsulinemia, hyperglycemia, and hyperlipidemia and markedly inhibits inflammation, fibrosis, and disruption of the islets in the genetically obese diabetic OLETF rats.
© 2005 Elsevier Inc. All rights reserved.

1. Introduction

The Otsuka Long-Evans Tokushima Fatty (OLETF) rat displays hyperphagia, obesity, hyperglycemia, hyperinsulinemia, and hyperlipidemia in early life [1]. During the hyperplastic stage, pancreatic islets of OLETF rats show islet enlargement with inflammatory cell infiltration and connective tissue proliferation [1-3]. During the chronic course of the hyperplastic stage, OLETF rats eventually become hypoinsulinemic and develop extreme atrophy of the pancreas and a significant reduction of the number and size of islets after 50 weeks of age [1-3].

Interleukin (IL) 1β, a proinflammatory cytokine, is induced in β cells of the gerbil *Psammomys obesus*, an animal model for type 2 diabetes [4], during the development of diabetes [5]. Moreover, treatment of rodent islets with IL-1β results in potent inhibition of insulin secretion followed by islet destruction [6,7]. On the other hand, recent studies have demonstrated that activation of pancreatic stellate cells (PSCs) plays an important role in the development of pancreatic fibrosis [2,7,8]. During pancreatic injury, PSCs are activated by proinflammatory cytokines such as tumor necrosis factor α (TNF-α), IL-1, and IL-6 [9] and transform into a myofibroblastic phenotype, exhibiting positive staining for α-smooth muscle actin (α-SMA), a marker of activated PSCs [2,8-10]. These results suggest that induction of IL-1β in the islets is involved in islet destruction and that activation of PSCs in response to proinflammatory

* Corresponding author. Tel.: +81 93 691 7251; fax: +81 93 692 0107.
E-mail address: mac-otsk@med.uoeh-u.ac.jp (M. Otsuki).

0026-0495/$ – see front matter © 2005 Elsevier Inc. All rights reserved.
doi:10.1016/j.metabol.2004.12.005

cytokines contributes to the development of pancreatic fibrosis and atrophy in OLETF rats [1-3].

Elevated levels of urokinase-type plasminogen activator (u-PA) are found in chronic pancreatitis, and such levels correlate with pancreatic damage [11]. It is supposed therefore that not only proinflammatory cytokines such as TNF-α, IL-1, and IL-6 but also u-PA are involved in the development of pancreatic fibrosis and atrophy in OLETF rats. Camostat, a synthetic protease inhibitor, is a potent inhibitor of trypsin as well as an inhibitor of inflammatory mediators such as plasmin, kallikrein (which enhances capillary permeability), thrombin, esterolytic activities of C1r and C1 esterase [12], and u-PA [13]. Camostat also inhibits proliferation and synthesis of collagen by human pancreatic periacinar fibroblastlike cells and hepatic stellate cells [14,15]. Several investigators have demonstrated that oral administration of camostat prevents the development of diabetes [16] and pancreatic fibrosis in WBN/Kob rats [17,18], a model of spontaneous chronic pancreatitis, through endogenous cholecystokinin (CCK) release [17] or through the suppression of gene expression of pancreatitis-associated protein, p8, and cytokines such as transforming growth factor β and IL-6 [18].

Considering the ability of camostat to modulate the inflammatory response and to inhibit fibrosis in the liver and pancreas [12,13,15-18], we undertook the present study to investigate whether long-term oral administration of camostat could delay or reverse the metabolic and histopathological changes in genetically obese and diabetic OLETF rats.

2. Materials and methods

2.1. Animals and diet

OLETF male rats aged 4 weeks were kindly supplied by the Tokushima Research Institute and maintained in a temperature (23°C ± 2°C)- and humidity (55% ± 5%)-controlled room with a 12/12-hour light/dark cycle (lights on at 7:00 AM). The animals were provided ad libitum with standard rat stock diet consisting of (as a percentage of calories) 61% carbohydrate, 26% protein, and 13% fat with cellulose (wt/wt) (3.596 kcal/g [15.046 kJ/g] diet; Oriental Yeast, Tokyo, Japan) and tap water. Rats were maintained according to the ethical guidelines of our institution, and the experimental protocol was approved by the animal welfare committee of our university.

2.2. Administration of camostat

Standard rat stock diet was pulverized to fine powder, and camostat (FOY-305, a generous gift from Ono Pharmaceutical, Osaka, Japan) was added and thoroughly mixed to a final concentration of 200 mg/100 g food. The drug-diet powder mixture was reconstituted into pellets of normal appearance. Diet for control rats was prepared in a similar fashion but without the addition of camostat.

2.3. Experimental protocol

OLETF rats were fed standard rat diet until the start of the experiment. They were divided at random into 3 groups. The first and the second groups of rats received camostat-rich diet from 12 weeks of age (before the onset of diabetes; F12-72) or from 28 weeks of age (after the onset of diabetes; F28-72) until the end of the study, whereas the third group of rats received standard rat diet free of camostat until the end of the study (control). All groups were allowed free access to food and water throughout the study. Animals were weighed on a weekly basis, and food intake was determined every 2 weeks over a 48-hour period by weighing the full food cups and then weighing the food cups again 48 hours later. The average food intake, after correction for spillage, was estimated as the amount of food consumed per cage. Feces were collected by using a metabolic cage over a 24-hour period, dried in oven, and weighed.

2.4. Intravenous glucose tolerance test

At 12, 20, 28, 36, 44, 52, 60, and 70 weeks of age, intravenous glucose tolerance test (IVGTT) was performed after an overnight fast. Animals were weighed before the experiments, and anesthesia was induced using sodium pentobarbital (50 mg/kg body weight, intraperitoneally). A bolus dose of glucose (200 mg/kg body weight) was injected into the right jugular vein immediately after blood sampling for measurement of serum concentrations of insulin, glucose, albumin, triglyceride (TG), free fatty acids (FFAs), and cholesterol. Blood samples were collected again from the left jugular vein at 5, 10, 30, and 60 minutes for measurement of serum concentrations of glucose and insulin.

2.5. Pancreas insulin content and adipose depots

Two weeks after the last IVGTT (72 weeks of age), rats were injected with sodium pentobarbital, and the abdomen was immediately opened. The retroperitoneal, mesenteric, and epididymal white adipose depots were dissected out and weighed. The pancreas was excised, cleared of surrounding lymph nodes and fat. Portions of each pancreatic tissue, with similar anatomic orientation, were used for histological examination. Pancreatic tissue was homogenized in saline using a motor-driven teflon-coated glass homogenizer at 3000 rpm (8 passes). The homogenates were filtered through 3 layers of gauze and then sonicated for 1 minute. Insulin was extracted by the modified method of Davoren [19].

2.6. Histological examination

A portion of the pancreatic tissue was fixed overnight in 4% paraformaldehyde solution for Azan staining and immunostaining and light-microscopic examination. All histological samples were examined in a single-blind fashion by the pathologist without awareness of the treatment group.

2.7. Quantitative analysis of pancreatic islet size

A portion of the pancreatic tissue was fixed overnight in 4% paraformaldehyde solution for hematoxylin and eosin staining, and the islet size in the pancreatic specimen was determined after pharmacological intervention with or without camostat using an Axiophot microscope (Carl Zeiss, Eching, Germany) connected to an interactive image analysis system (IBAS, Carl Zeiss). Ten nonoverlapping fields per hematoxylin-eosin–stained pancreatic specimen (n = 6-8, at each time point) were randomly selected at ×100 magnification. The islet area (μm^2) was determined by using the IBAS image analysis system.

2.8. Immunohistochemistry

Paraffin-embedded pancreatic tissue sections were prepared on glass slides. Sections for IL-1β and IL-6 immunohistochemistry were pretreated in microwaves in citrate buffer (pH 6.0) for 12 minutes, whereas sections for TNF-α immunohistochemistry were incubated in proteinase K for 10 minutes (for antigen retrieval). These prepared sections were incubated for 15 minutes in 3% H_2O_2 to block endogenous peroxidase activities. Nonspecific staining was blocked by incubation with bovine normal serum for 10 minutes at room temperature. Each section was incubated with anti–TNF-α antibody (Santa Cruz Biotechnology, Inc, Santa Cruz, Calif), anti–IL-1β antibody (Santa Cruz Biotechnology, Inc), or anti–IL-6 antibody (Santa Cruz Biotechnology, Inc) at 1:10 dilution for 60 minutes at room temperature. Sections prepared for α-SMA immunohistochemistry were incubated with anti–α-SMA antibody (Dako Corporation, Carpinteria, Calif) at 1:50 dilution for 30 minutes at room temperature. Bound antibodies were detected with the peroxidase-labeled streptavidin-biotin method (LSAB Kit; Dako Corporation) and stained with diaminobenzidine. Finally, the sections were counterstained with Mayer hematoxylin and mounted.

2.9. Assays

Serum glucose concentrations were determined by the glucose-oxidase method using a glucose kit (Glucose-E reagent; International Reagents, Kobe, Japan). Insulin concentrations in the serum and pancreatic homogenates were measured by radioimmunoassay using the double-antibody method with a commercially available kit (ShionoRIA; Shionogi Pharmaceutical, Osaka) using crystalline rat insulin as a reference standard. Serum albumin, TG, FFAs, and cholesterol concentrations were determined with the Hitachi 736 automatic analyzer system (Hitachi, Tokyo). DNA concentrations in pancreatic homogenates were determined by the method of Labarca and Paigen [20] using the fluorescent dye H-33258 (Hoechst, Frankfurt, Germany) and calf thymus DNA (type 1; Sigma Chemical, St Louis, Mo) as a standard. Protein content in feces was measured by the method of Wagner [21].

Insulin sensitivity was calculated by homeostasis model assessment insulin resistance (HOMA-IR) using the following formula: fasting insulin (microunits per milliliters) × fasting glucose (mmol/L)/22.5, as described by Matthews et al [22]. According to this method, low HOMA scores denote high insulin sensitivity (low insulin resistance) [22]. Because the HOMA-IR is based on fasting insulin and glucose concentrations, there are limitations to the HOMA-IR method. Fukushima et al [23] reported that HOMA-IR values correlate significantly with insulin resistance calculated by the minimal model approach in subjects with varying degrees of glucose tolerance.

2.10. Statistical analysis

Results are presented as mean ± SEM. Differences between groups were tested for statistical significance using analysis of variance followed by Tukey test. A P value less than .05 denoted a statistically significant difference.

3. Results

3.1. Food consumption, body weight, and adipose depots

We first assessed whether camostat alters food and calorie intake, nutritional status, and body weight compared with

Table 1
Effects of camostat on food and calorie intake, and fecal protein excretion in OLETF rats at 49 weeks of age

	Control (n = 6)	F12-72 (n = 8)	F28-72 (n = 7)
Body weight (g)	699 ± 13	546 ± 7[a]	536 ± 15[a]
Food intake			
g/d per rat	30.0 ± 0.4	31.0 ± 0.9	31.1 ± 0.5
g/100-g body weight per day	4.29 ± 0.06	5.68 ± 0.16[a]	5.80 ± 0.09[a]
Estimated calorie intake			
kcal/d per rat	107 ± 2	110 ± 4	110 ± 2
kJ/rat per day	448 ± 8	460 ± 17	460 ± 8
kcal/100-g body weight per day	15.3 ± 0.2	20.1 ± 0.6[a]	20.5 ± 0.3[a]
kJ/100 g body weight per day	64.0 ± 0.8	84.1 ± 2.5[a]	85.8 ± 1.3[a]
Fecal protein content (g/d per rat)	1.7 ± 0.1	5.8 ± 0.8[a]	5.9 ± 0.6[a]
Estimated calorie loss based on fecal protein			
kcal/d per rat	6.8 ± 0.4	23.2 ± 3.3[a]	23.6 ± 2.5[a]
kJ/rat per day	28.5 ± 1.7	97.1 ± 13.8[a]	98.7 ± 10.5[a]
kcal/100-g body weight per day	0.97 ± 0.06	4.25 ± 0.59[a]	4.40 ± 0.45[a]
kJ/100 g body weight per day	4.1 ± 0.3	17.8 ± 2.5[a]	18.4 ± 1.9[a]
Calorie loss (%): estimated calorie loss based on fecal protein/ estimated calorie intake	6.3 ± 0.5	21.1 ± 2.4[a]	21.5 ± 1.9[a]
Calorie intake: estimated calorie intake – estimated calorie loss in feces			
kcal/100 g body weight per day	14.7 ± 0.2	15.6 ± 0.6	15.6 ± 0.3
kJ/100 g body weight per day	61.5 ± 0.8	65.3 ± 2.5	65.3 ± 1.3
Serum albumin (g/100 mL)	3.93 ± 0.04	4.00 ± 0.05	4.07 ± 0.04

Values are mean ± SEM of the indicated number of rats. Treatment groups were similar to those indicated in Fig. 1. Rats were treated with camostat from 12 or 28 weeks of age to 72 weeks of age (F12-72 and F28-72).

[a] Significantly different from the control.

Table 2
Effects of camostat-treatment on body weight, adipose depot, and pancreatic insulin content in OLETF rats at 72 weeks of age

Parameters	Control (n = 6)	F12-72 (n = 8)	F28-72 (n = 7)
Body weight (g)	726 ± 15	574 ± 7[a]	536 ± 15[a]
White adipose tissue (mesenteric + retroperitoneal + epididymal)			
grams per rat	105.2 ± 7.3	47.8 ± 3.1[a]	42.7 ± 3.9[a]
mg/g body weight	150.5 ± 8.4	88.6 ± 4.8[a]	82.7 ± 6.1[a]
Pancreatic insulin content			
nmol/pancreas	10.3 ± 1.2	24.2 ± 1.2[a]	24.0 ± 1.0[a]
nmol/mg DNA	1.79 ± 0.33	3.21 ± 0.09[a]	3.23 ± 0.18[a]
Serum concentrations			
Glucose (mmol/L)	14.2 ± 0.9	9.3 ± 0.3[a]	8.8 ± 0.4[a]
Insulin (pmol/L)	276 ± 22	356 ± 25[a]	325 ± 13[a]
TG (mmol/L)	3.91 ± 0.12	1.19 ± 0.02[a]	1.12 ± 0.01[a]
Cholesterol (mmol/L)	4.86 ± 0.22	2.17 ± 0.13[a]	2.25 ± 0.21[a]
FFAs (g/L)	0.36 ± 0.02	0.10 ± 0.01[a]	0.12 ± 0.01[a]

Values are mean ± SEM of the indicated number of rats.
Treatment groups were similar to those indicated in Fig. 1. Rats were treated with camostat from 12 or 28 weeks of age to 72 weeks of age (F12-72 and F28-72).
[a] Significantly different from the control.

standard diet. Food intake of untreated control rats gradually increased from 27.3 ± 0.3 g/d per rat at 12 weeks of age to 30.8 ± 0.5 g/d per rat at 16 weeks and remained at this level until 70 weeks of age. However, when food intake was adjusted for body weight, it showed a gradual decrease with age (12 vs 70 weeks of age; 6.71 ± 0.07 vs 4.19 ± 0.07 g/100-g body weight per day, $P < 0.01$). The daily amount of food intake per rat in treated rats was similar to that in untreated control rats, but that adjusted for body weight was significantly higher in treated rats than in untreated control rats (Table 1). Although the estimated calorie loss based on fecal protein in treated rats was approximately 15% greater than in untreated rats, there was no significant difference in calorie intake calculated from food intake and fecal protein loss adjusted for body weight between treated and untreated rats. Serum albumin concentrations in the camostat-fed rats were similar to those in untreated control rats (Table 1), suggesting that camostat does not cause malnutrition.

Body weight of the control rats increased progressively with age. The addition of camostat to the diet from 12 weeks of age (F12-72) diminished the gain in body weight (Table 2), whereas when it was added from 28 weeks of age (F28-72), it reduced body weight from 596 ± 10 g at 28 weeks of age to 555 ± 6 g at 36 weeks of age ($P < .01$), and the body weight remained at nearly the same level until the end of the study. Camostat treatment significantly reduced total adipose depots (mesenteric, retroperitoneal, and epididymal) (Table 2).

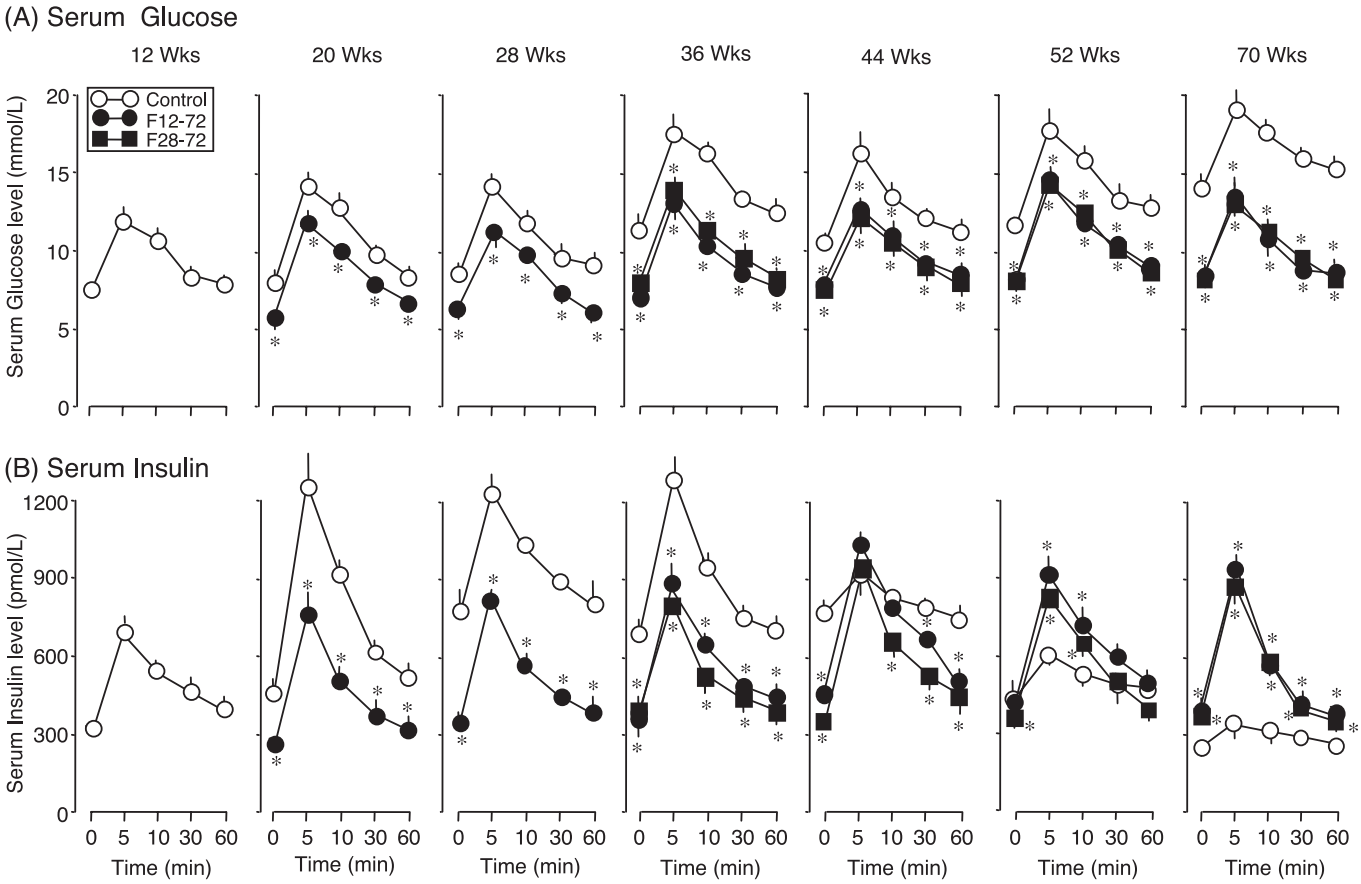

Fig. 1. Serial changes in serum glucose (A) and insulin (B) responses to an intravenous glucose load in control and camostat-treated OLETF rats (F12-72 and F28-72). Control rats fed a camostat-free standard rat diet until the end of the study; F12-72, OLETF rats were fed camostat-containing diet from 12 weeks of age, before the onset of diabetes, until the end of the 72-week study; F28-72, OLETF rats fed camostat-containing diet from 28 weeks of age, after the onset of diabetes, until the end of the 72-week study. Results are mean ± SEM of 6 to 8 rats. *Significant difference versus control at the corresponding time point.

3.2. Serum insulin and glucose response to IVGTT, insulin resistance, and pancreatic insulin content

We then assessed whether camostat affected glucose homeostasis. In the control rats, the glycemic response to IVGTT as well as fasting serum glucose concentrations gradually increased with age (Fig. 1A). Camostat inhibited (F12-72) or normalized (F28-72) the fasting serum glucose concentrations and maintained the dynamic response at levels similar to those observed at 12 weeks of age until 70 weeks of age.

To determine whether the difference in glucose tolerance was associated with an altered β-cell response, we measured insulin secretion before and after glucose injection. Basal serum insulin levels in the control rats increased significantly with age until 44 weeks of age, but they progressively decreased thereafter (Fig. 1B). Insulin secretion in response to IVGTT significantly increased in the control rats until 36 weeks of age, but it showed no significant increases after 44 weeks of age. Camostat treatment prevented or improved the fasting serum insulin levels and maintained insulin response to glucose injection at levels similar to those observed at 12 weeks of age until the end of the study. We then evaluated insulin resistance by HOMA-IR, as described by Matthews et al [22]. HOMA-IR progressively increased up to age 52 weeks, and such increase correlated with increases in fasting glucose and insulin concentrations, but it rapidly decreased thereafter in association with decreases in fasting serum insulin levels (Fig. 2). Although there are limitations to the HOMA-IR method, which is only based on fasting insulin and glucose concentrations, treatment with camostat prevented the increase (F12-72) or significantly reduced (F28-72) HOMA-IR to that at 12 weeks of age until the end of the study. Therefore, camostat treatment prevented the increase in insulin resistance. Camostat also increased insulin content in the pancreas by approximately 2-fold irrespective of whether it was expressed as the total amount or related to DNA content (Table 2).

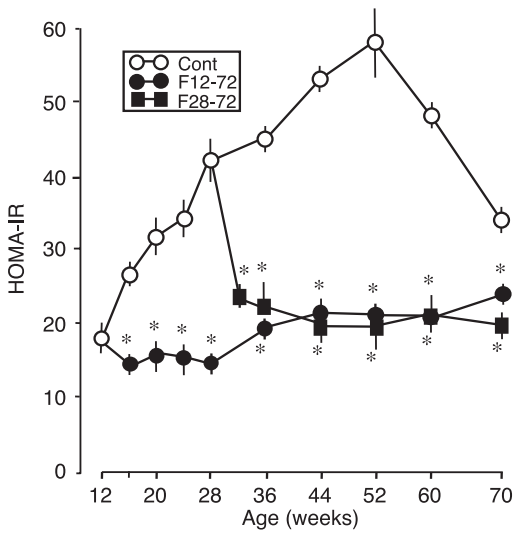

Fig. 2. Serial changes in HOMA-IR in control and camostat-treated OLETF rats (F12-72 and F28-72). For explanation of the different experimental groups, see the legend for Fig. 1. Results are mean ± SEM of 6 to 8 rats. *Significant difference versus control at the same age.

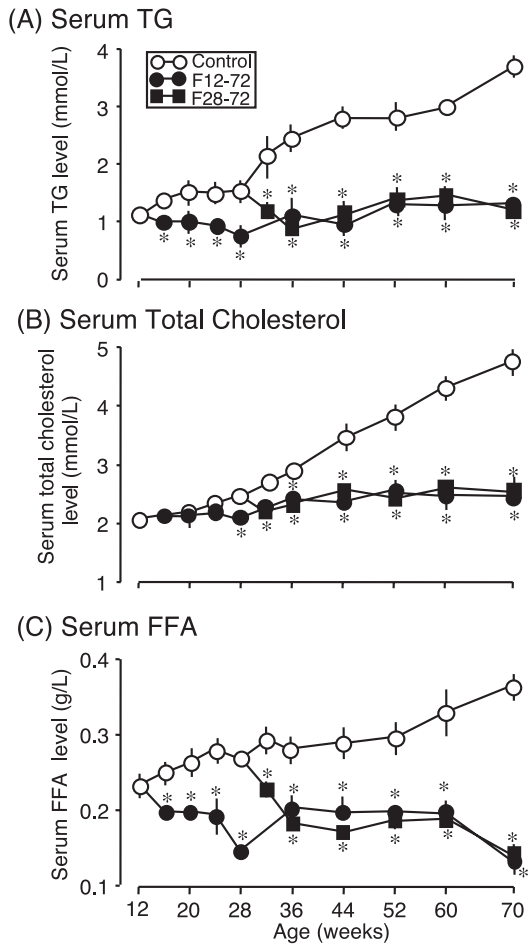

Fig. 3. Serial changes in fasting serum TG (A), cholesterol (B), and FFAs (C) in control and camostat-treated OLETF rats (F12-72 and F28-72). For explanation of the different experimental groups, see the legend for Fig. 1. Results are mean ± SEM of 6 to 8 rats. *Significant difference versus control at corresponding age.

3.3. Fasting serum levels of TG, cholesterol, and FFAs

We then assessed whether camostat affects serum lipids levels compared with standard diet. Fasting serum concentrations of TG, cholesterol, and FFAs increased progressively with age in untreated control rats (Fig. 3). Treatment with camostat from 12 (F12-72) or 28 (F28-72) weeks of age prevented the increase in cholesterol and significantly reduced the serum concentrations of TG and FFAs. After 36 weeks of age, there were no significant differences in serum levels of lipids between the 2 treatment groups (F12-72 vs F28-72).

3.4. Histopathological changes

We also investigated whether the differences in glucose tolerance and lipid metabolism were associated with improvement in pancreatic histology. In untreated control OLETF rats, islet size at 28 weeks of age was approximately

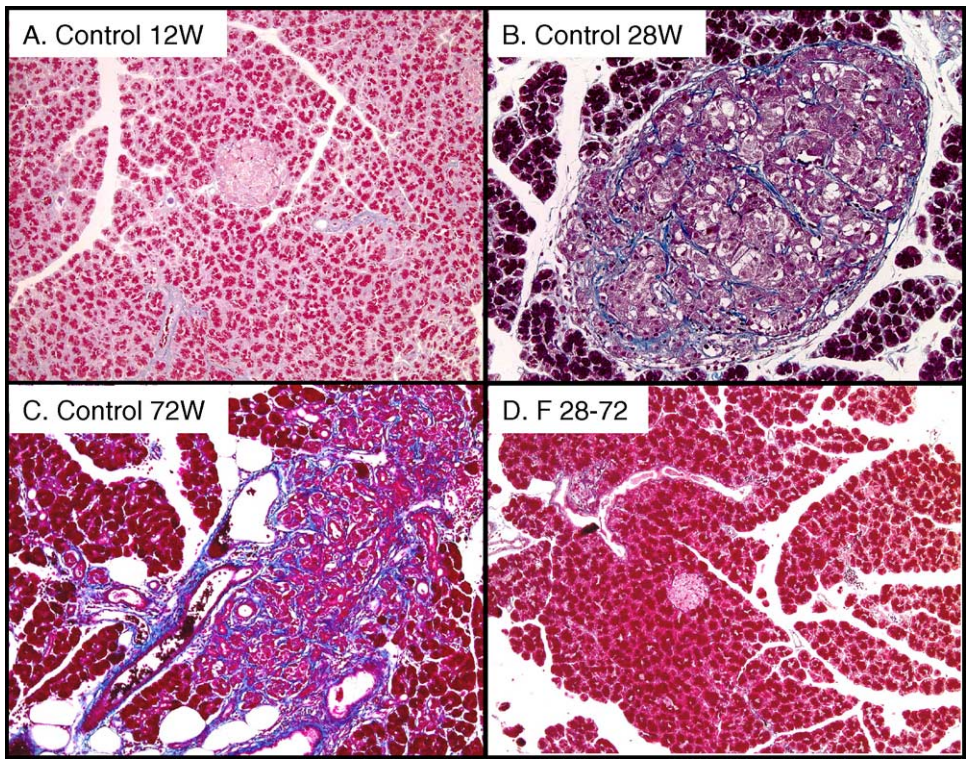

Fig. 4. Representative photomicrographs of Azan-stained pancreas of control rats at age 12 (A), 28 (B), and 72 (C) weeks of age and camostat-treated OLETF rat (D). In the control rats, islet was enlarged with irregular boundaries at 28 weeks of age (B), or it showed extreme atrophy and replacement of normal tissue by fatty and connective tissue at 72 weeks of age (C). Camostat treatment from 28 to 72 weeks' age reversed and prevented these histopathological alterations in the pancreas (D). Original magnification ×50.

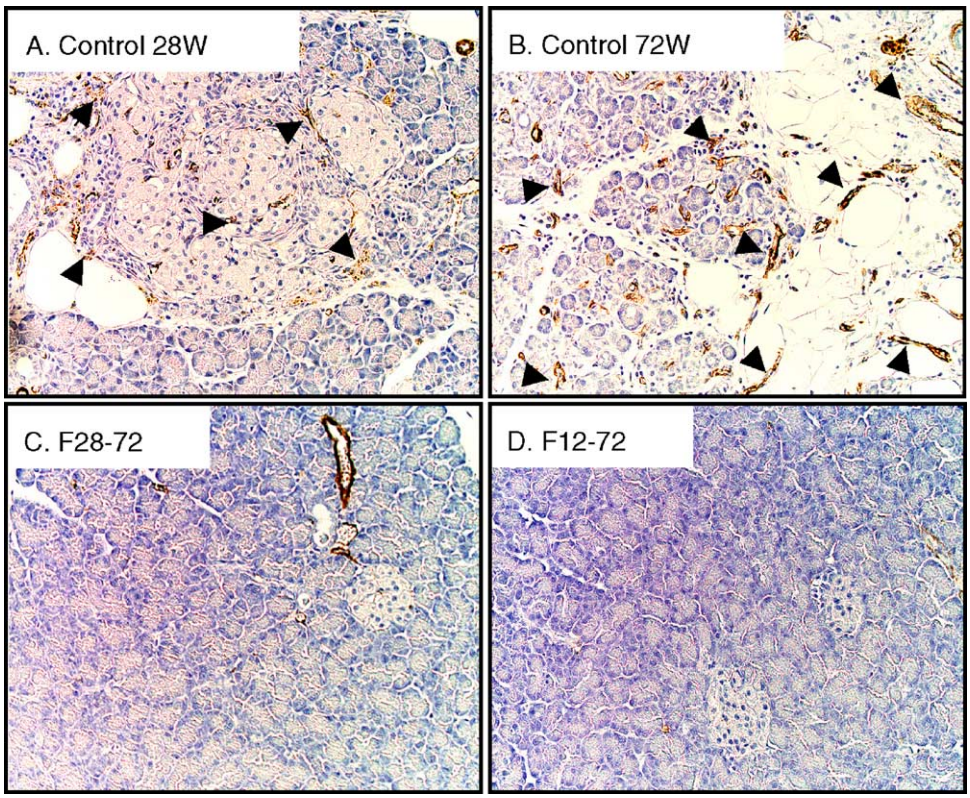

Fig. 5. Representative photomicrographs showing pancreatic α-SMA expression examined by immunohistochemistry at 28 and 72 weeks of age. A, B, In the control rats, α-SMA was strongly expressed in the fibrotic or degenerative regions of pancreatic islets (A, 28 weeks of age; B, 72 weeks of age). Camostat treatment suppressed the expression of α-SMA (C, F28-72; D, F12-72). Original magnification ×50.

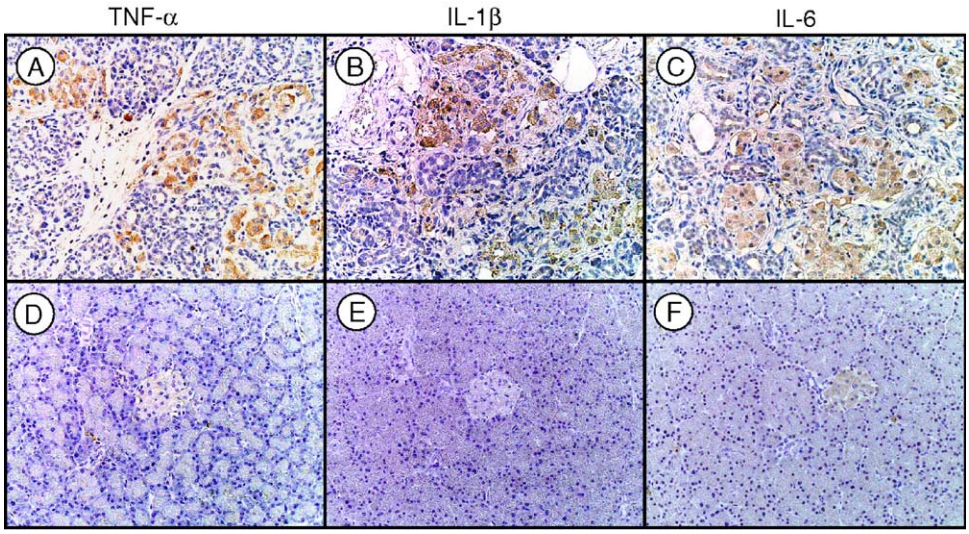

Fig. 6. Representative photomicrographs showing immunohistochemical staining for TNF-α, IL-1β and IL-6 in the pancreas at 72 weeks of age. In control rats, TNF-α (A), IL-1β (B) and IL-6 (C) were strongly expressed in the fibrotic or degenerative regions of endocrine pancreas. In camostat-treated rats, the expression levels of TNF-α (D, F28-72), IL-1β (E, F28-72), and IL-6 (F, F28-72) were almost completely suppressed. Original magnification ×50.

3.5 times larger than that at 12 weeks of age (Figs. 4A vs B, 12 vs 28 weeks of age; 678 ± 96 vs 2130 ± 68 μm^2, $P < .001$). At 72 weeks of age, the pancreas of untreated control OLETF rats was extremely atrophic, and both the number and size of islets were significantly reduced. Because the contour of the islets was irregular with structural disarrangement and fibrosis, and the islets were separated into small sections (cluster) by fibrosis (Fig. 4C), we could not determine islet size in these rats. Treatment with camostat prevented the increase in islet size when such treatment was initiated before enlargement of islet size (F12-72 vs 12 weeks of age; 652 ± 78 vs 678 ± 96 μm^2, NS) and completely normalized the islets size when the treatment commenced after islet hypertrophy (Fig. 4B vs D, control at 28 weeks of age vs F28-72; 2130 ± 68 vs 782 ± 79 μm^2, $P < .001$, 12 weeks of age vs F28-72, NS). Moreover, α-SMA, a marker of activated PSCs that are involved in pancreatic fibrosis [2,8-10], was strongly expressed in the fibrotic and degenerative regions of the islets at 28 weeks of age (Fig. 5A), and its expression was further increased at 72 weeks of age (Fig. 5B). Moreover, camostat treatment prevented the appearance of α-SMA–positive cells (F12-72) (Fig. 5C) and also resulted in their disappearance in the islets (F28-72) (Figs. 5D vs A). At 72 weeks of age, the untreated control OLETF rats showed strong expression of TNF-α (Fig. 6A), IL-1β (Fig. 6B), and IL-6 (Fig. 6C) in the fibrotic and degenerative regions of the endocrine pancreas, whereas camostat treatment almost completely suppressed the expression of these cytokines (Figs. 6D, E, F).

4. Discussion

Our study demonstrated that treatment of the genetically obese and diabetic OLETF rats with synthetic trypsin inhibitor camostat not only prevented but also improved metabolic derangement such as hyperglycemia, hyperinsulinemia, hyperlipidemia and obesity, and the size and characteristic histopathological changes of the islets to near-normal up to 72 weeks of age.

Oral administration of camostat stimulates endogenous CCK release by inhibiting trypsin activity in the small intestine [24]. Sugiyama et al [17] demonstrated that oral administration of camostat has both preventive and therapeutic effects on pancreatic lesions such as inflammatory cell infiltration and fibrosis, and pancreatic exocrine dysfunction in WBN/Kob rats, an animal model of spontaneous chronic pancreatitis, via endogenous CCK release. However, OLETF rats are genetically deficient of CCK-1 receptors mRNA [25], and the exocrine and endocrine pancreas as well as satiety center are totally and specifically insensitive to exogenous and endogenous CCK stimulation [25-27]. Therefore, it is unlikely that the effects of camostat on the pancreas of OLETF rats are mediated through the release of endogenous CCK.

Although the major effect of camostat appears to be wasting of protein in the feces, resulting in calorie loss and reduction of weight gain, camostat-treated rats consumed more food than the control rats when food intake was adjusted for body weight. Moreover, there was no significant difference in calorie intake adjusted for body weight in spite of larger protein loss in feces. In keeping with this, serum albumin levels in camostat-treated rats were not significantly different from those in control rats. These results, together with the observations that camostat strongly inhibits trypsin but has no effects on other digestive enzymes [11], indicate that camostat might have caused mainly energy deficiency with limited associated protein malnutrition.

Obesity is considered to be a potent diabetogenic factor. Adipose tissue produces and secretes a large number of hormones, cytokines, and proteins that affect glucose

homeostasis and insulin sensitivity, including leptin, TNF-α, peroxisome proliferator-activated receptor (PPAR) γ, resistin, and adiponectin [28,29]. Previous studies have shown that reduction of body weight by caloric restriction [30-32], surgical removal of intra-abdominal fat pads [33,34], or oral administration of α-glucosidase inhibitor acarbose [35,36] results in improvement of insulin actions in obese rodent models including OLETF rats. Therefore, it is possible that the effects of camostat in OLETF rats observed in the present study are based on weight loss or failure of weight gain. However, several studies have demonstrated that oral administration of camostat prevents the development of diabetes and pancreatic fibrosis in WBN/Kob rats without affecting [16,17] or even increasing body weight [18]. Moreover, we have found in our previous studies that impairment of insulin secretion appears before the onset of abnormal lipid metabolism in OLETF rats [3,35]. Although these results suggest that the effects of camostat in OLETF rats are unlikely to be solely caused by weight loss or failure of weight gain, it is difficult to rule out the scenario of camostat-induced reduction of visceral adipose deposits as a cause of improved β-cell function. The reduced increase of blood glucose and insulin resistance, the low rate of weight gain, and reduced visceral adipose depots in camostat-treated OLETF rats might help maintain β-cell function and prevent enlargement or atrophy of the islets by protecting β cells from overactivity and exhaustion.

Camostat suppresses not only proteases but also inflammatory mediators and free radical activity [11,12,37]. Recent studies have demonstrated that camostat inhibits the proliferation and collagen synthesis by pancreatic periacinar fibroblastlike cells and hepatic stellate cells [14,15]. Moreover, camostat inhibits inflammatory changes and fibrosis of the pancreas through the suppression of gene expression of pancreatitis-associated protein, p8, and cytokines including IL-6 [18] and improves pancreatic exocrine and endocrine functions in WBN/Kob rats [16,17]. Consistent with these observations, oral administration of camostat strongly inhibited pancreatic fibrosis; expressions of α-SMA, TNF-α, IL-1β, and IL-6; and infiltration of inflammatory cells in the pancreas of OLETF rats. In addition, treatment with camostat greatly improved insulin resistance evaluated by HOMA-IR and the islet size evaluated by the IBAS image analysis system until the end of the study at 72 weeks of age. Of special interest is that camostat improved all parameters examined in the present study to the same levels irrespective of whether the treatment commenced before (F12-72) or after (F28-72) the onset of diabetes. Based on the present results, we propose that camostat acts as an anti-inflammatory agent in the pancreas of diabetic OLETF rats by regulating proinflammatory cytokines such as TNF-α, IL-1β, and IL-6, although the present study did not categorically confirm this proposal and exclude the effect of weight loss.

In our long-term study of genetically obese and diabetic OLETF rats, a model of spontaneous type 2 diabetes, pharmacological intervention with camostat not only prevented the development of obesity and diabetes when given before the onset of diabetes but also reversed hyperglycemia, dyslipidemia, obesity, and histological alterations of the pancreas and improved insulin resistance even when given after the onset of diabetes. We conclude that camostat is beneficial for both prevention and resolution of obesity and diabetes in this model.

Acknowledgment

The authors thank Dr Hiroyuki Yoshikawa for the excellent technical assistance. This research was supported in part by Grants-in-aid for Scientific Research (10470144) from the Ministry of Education, Science, Sports, and Culture, Japan, and the Japanese Ministry of Health and Welfare (Intractable Diseases of the Pancreas).

References

[1] Kawano K, Hirashima T, Mori S, et al. Spontaneous long-term hyperglycemic rat with diabetic complications. Otsuka Long-Evans Tokushima Fatty (OLETF) strain. Diabetes 1992;41:1422-8.
[2] Yoshikawa H, Kihara Y, Taguchi M, et al. Role of TGF-β1 in the development of pancreatic fibrosis in Otsuka Long-Evans Tokushima Fatty rats. Am J Physiol Gastrointest Liver Physiol 2002;282:G549-58.
[3] Jia DM, Fukumitsu KI, Tabaru A, et al. Troglitazone stimulates pancreatic growth in congenitally CCK-A receptor–deficient OLETF rats. Am J Physiol 2001;280:R1332-40.
[4] Kalderon B, Gutman A, Levy E, et al. Characterization of stages in development of obesity-diabetes syndrome in sand rat (*Psammomys obesus*). Diabetes 1986;35:717-24.
[5] Maedler K, Sergeev P, Ris F, et al. Glucose-induced beta cell production of IL-1β contributes to glucotoxicity in human pancreatic islets. J Clin Invest 2002;110:851-60.
[6] Mandrup-Poulsen T, Bendtzen K, Nielsen JH, et al. Cytokines cause functional and structural damage to isolated islets of Langerhans. Allergy 1985;40:424-9.
[7] Apte M, Haber P, Applegate T, et al. Periacinar stellate shaped cells in rat pancreas: Identification, isolation, and culture. Gut 1998;43:128-33.
[8] Bachem M, Schneider E, Grob H, et al. Identification, culture, and characterisation of pancreatic stellate cells in rats and humans. Gastroenterology 1998;115:421-32.
[9] Formela L, Galloway S, Kingsnorth A. Inflammatory mediators in acute pancreatitis. Br J Surg 1995;85:6-13.
[10] Haber P, Keogh G, Apte M, et al. Activation of pancreatic stellate cells in human and experimental pancreatic fibrosis. Am J Pathol 1999;155:1087-95.
[11] Friess H, Cantero D, Graber H, et al. Enhanced urokinase plasminogen activation in chronic pancreatitis suggests a role in its pathogenesis. Gastroenterology 1997;113:904-13.
[12] Tamura Y, Hirado M, Okamura K, et al. Synthetic inhibitor of trypsin, plasmin, kallikrein, thrombin, C1r and C1 esterase. Biochim Biophys Acta 1977;484:417-22.
[13] Ikeda T, Murakami K, Hayakawa Y, et al. Anti-invasive activity of synthetic serine protease inhibitors and its combined effect with a matrix metalloproteinase inhibitor. Anticancer Res 1998;18:4259-65.
[14] Nakamura F, Shintani Y, Saotome T, et al. Effects of synthetic serine protease inhibitors on proliferation and collagen synthesis of human pancreatic periacinar fibroblast-like cells. Pancreas 2001;22:317-25.
[15] Okuno M, Akita K, Moriwaki H, et al. Prevention of rat hepatic fibrosis by the protease inhibitor, camostat mesilate, via reduced generation of active TGF-β. Gastroenterology 2001;120:1784-800.

[16] Shimoda I, Koizumi M, Shimosegawa T, et al. Physiological characteristics of spontaneously developed diabetes in chronic oral administration of synthetic trypsin inhibitor (FOY-305). Pancreas 1993;8: 196-203.
[17] Sugiyama M, Kobori O, Atomi Y, et al. Effect of oral administration of protease inhibitor on pancreatic exocrine function in WBN/Kob rats with chronic pancreatitis. Pancreas 1996;13:71-9.
[18] Su SB, Motoo Y, Iovanna JL, et al. Effect of camostat mesilate on the expression of pancreatitis-associated protein (PAP), p8, and cytokines in rat spontaneous chronic pancreatitis. Pancreas 2001;23:134-40.
[19] Davoren PR. The isolation of insulin from a single cat pancreas. Biochim Biophys Acta 1962;63:150-3.
[20] Labarca C, Paigen K. A simple, rapid and sensitive DNA assay procedure. Anal Biochem 1980;102:344-52.
[21] Wagner A. On the quantitative determination of fecal proteins. Klin Wochenschr 1967;45:1056.
[22] Matthews DR, Hosker JP, Rudenski AS, et al. Homeostasis model assessment: Insulin resistance and B-cell function from fasting plasma glucose and insulin concentrations in man. Diabetologia 1985;28: 412-9.
[23] Fukushima M, Taniguchi A, Sakai M, et al. Homeostasis model assessment as a clinical index of insulin resistance. Comparison with the minimal model analysis. Diabetes Care 1999;22:1911-2.
[24] Fukumitsu K, Nakamura H, Otsuki M. Oral administration of protease inhibitor decreases CCK-A receptor mRNA expression but increases pancreatic growth in rats. Pancreas 2001;22:179-85.
[25] Nakamura H, Kihara Y, Tashiro M, et al. CCK-A receptor–mediated biological functions in Otsuka Long-Evans Tokushima Fatty (OLETF) rats. J Gastroenterol 1998;33:702-9.
[26] Moran TH, Katz LF, Plata-Salaman CR, et al. Disordered food intake and obesity in rats lacking cholecystokinin receptors. Am J Physiol 1998;274:R618-25.
[27] Otsuki M, Akiyama T, Shirohara H, et al. Loss of sensitivity to cholecystokinin stimulation of isolated pancreatic acini from genetically diabetic rats. Am J Physiol 1995;268:E531-6.
[28] Spiegelman BM, Flier JS. Adipogenesis and obesity: Rounding out the big picture. Cell 1996;87:377-89.
[29] Saltiel AR. New perspectives into the molecular pathogenesis and treatment of type 2 diabetes. Cell 2001;104:517-29.
[30] Okauchi N, Mizuno A, Yoshimoto S, et al. Is caloric restriction effective in preventing diabetes mellitus in the Otsuka Long-Evans Tokushima Fatty rat, a model of spontaneous non–insulin-dependent diabetes mellitus? Diabetes Res Clin Pract 1995;27:97-106.
[31] Walder K, Dascaliuc CR, Lewandowski PA, et al. The effect of dietary energy restriction on body weight gain and the development of noninsulin-dependent diabetes mellitus (NIDDM) in *Psammomys obesus*. Obes Res 1997;5:193-200.
[32] Barzilai N, Banerjee S, Hawkins M, et al. Caloric restriction reverses hepatic insulin resistance in aging rats by decreasing visceral fat. J Clin Invest 1998;101:1353-61.
[33] Kim YW, Kim JY, Lee SK. Surgical removal of visceral fat decreases plasma free fatty acid and increases insulin sensitivity on liver and peripheral tissue in monosodium glutamate (MSG)–obese rats. J Korean Med Sci 1999;14:539-45.
[34] Barzilai N, She L, Liu BQ, et al. Surgical removal of visceral fat reverses hepatic insulin resistance. Diabetes 1999;48:94-8.
[35] Yamamoto M, Jia DM, Fukumitsu K, et al. Metabolic abnormalities in the genetically obese and diabetic Otsuka Long-Evans Tokushima Fatty rat can be prevented and reversed by α-glucosidase inhibitor. Metabolism 1999;48:347-54.
[36] Carrascosa JM, Molero JC, Fermin Y, et al. Effects of chronic treatment with acarbose on glucose and lipid metabolism in obese diabetic Wistar rats. Diabetes Obes Metab 2001;3:240-8.
[37] Manabe T, Asano N, Yoshimura T, et al. Effect of synthetic protease inhibitor on histologic changes and free radical activity in hamsters with pancreatic cancer. Scand J Gastroenterol 1993;28:719-24.